29. J. M. Besterman, S. P. Watson, P. Cuatrecasas, *ibid.*, p. 723.
30. S. Palmer *et al.*, *Biochem J.* **238**, 491 (1986).
31. M.R. is the recipient of a grant from Associazione Italiana per la Ricerca sul Cancro. We thank Charles Knicley and Claire Pennington for technical assistance.

8 September 1987; accepted 11 December 1987

Replacements of Pro^{86} in Phage T4 Lysozyme Extend an α-Helix But Do Not Alter Protein Stability

TOM ALBER, JEFFREY A. BELL, SUN DAO-PIN, HALE NICHOLSON, JOAN A. WOZNIAK, SEAN COOK, BRIAN W. MATTHEWS

To investigate the relation between protein stability and the predicted stabilities of individual secondary structural elements, residue Pro^{86} in an α-helix in phage T4 lysozyme was replaced by ten different amino acids. The x-ray crystal structures of seven of the mutant lysozymes were determined at high resolution. In each case, replacement of the proline resulted in the formation of an extended α-helix. This involves a large conformational change in residues 81 to 83 and smaller shifts that extend 20 angstroms across the protein surface. Unexpectedly, all ten amino acid substitutions marginally reduce protein thermostability. This insensitivity of stability to the amino acid at position 86 is not simply explained by statistical and thermodynamic criteria for helical propensity. The observed conformational changes illustrate a general mechanism by which proteins can tolerate mutations.

A MAJOR PROBLEM IN UNDERSTANDING the physical basis of protein stability is to quantitate the contributions made by specific interactions observed in the folded structure (*1, 2*). One aspect of this general problem is to determine how the amino acid sequence establishes the stability of α-helices and other secondary structures (*3–10*). The stabilizing contribution of each secondary structural element might then be understood as a product of its intrinsic stability and its affinity for the remainder of the protein (*5*). To systematically investigate the relation between protein thermostability and the predicted stability of individual secondary structural elements, we replaced a proline in a helix in phage T4 lysozyme with ten other amino acids.

A degenerate oligonucleotide mixture was used to simultaneously create several amino acid substitutions at position 86 (*6, 11*). A mutagenic 22-base primer specifying all four nucleotides (N) in the first two positions and thymine (T) in the third position of the CCG codon for Pro^{86} was used in the two-primer protocol of Zoller and Smith (*12*). This combination of sequences, NNT, encodes 15 different amino acids including proline. By virtue of the mismatch in the third position of codon 86 (T ≠ G), mutants could be distinguished from wild-type (WT) clones by differential hybridization to the ^{32}P-labeled mutagenic oligonucleotide mixture (*12*). Of the 14 possible amino acid substitutions, 10 specified by the primer were identified by DNA sequencing (*13*), namely Ser, Thr, Cys, Ala, Gly, Leu, Ile, His, Arg, and Asp.

The mutant lysozyme genes were subcloned into the expression vector pHSe5 and the mutant proteins were purified to homogeneity by ion exchange chromatography on CM-Sephadex. The protein samples each produced a single band on an SDS-polyacrylamide gel stained with silver (*14, 15*).

The effect of each substitution at Pro^{86} on the thermodynamic stability of the protein was assessed by monitoring the circular dichroism at 223 nm as a function of temperature (*16*). The changes in melting temperature, T_m, are listed in Table 1. The stability of the enzyme is surprisingly insensitive to these mutations. With the exception of Pro^{86} → Asp, which is almost indistinguishable from wild-type T4 lysozyme, all of the mutant proteins are marginally destabilized. Using the relation $g_0 = -T\Delta S$ (*17*), the reductions in stability were estimated to be less than 0.5 kcal/mol at 42°C.

The stabilities of the mutant proteins do not rank according to the helix propensity, P_α (*3*), or the helix-coil stability constant, s (*4*), of the amino acid at position 86 (Table 1). In addition, the observed changes in stability are smaller in magnitude than the reported changes due to mutations in helices of λ repressor (*7*), staphylococcal nuclease (*8*), and in other helices of T4 lysozyme (*6*).

The substitutions at position 86 cause more obvious changes in enzymatic activity (*18*) than in protein stability (Table 1). At *p*H 6.8, the protein containing Arg^{86} has one-fifth the activity of the wild type enzyme and the protein with Asp^{86} is 10% more active than the wild type. These results suggest that the catalytic efficiency is sensitive to the charge of residue 86, despite the fact that this site is ~24 Å from the scissile bond.

Mutant lysozymes were crystallized under conditions similar to those for the wild-type enzyme and equilibrated with *p*H 6.7 mother liquor prior to data collection (*19*). Variants with Gly, Ser, Cys, Leu, Asp, Arg, and His at position 86 were used to obtain x-ray data to 1.7 to 1.9 Å resolution by oscillation photography (*20*) (Table 2). Electron densi-

Table 1. Properties of wild-type (Pro^{86}) and mutant T4 lysozymes. T_m is the temperature at the midpoint of the reversible thermal denaturation transition measured by the method in (*16*). The protein concentration was 30 μg/ml. P_α is the normalized frequency of occurrence in α-helices from (*3*), and s is the helix propagation constant at 20°C from (*4*).

Residue 86	T_m (1°C)			Relative specific activity*	Average *B*-value of residue 86 side chain (Å^2)	P_α	s
	*p*H 2	*p*H 4	*p*H 6				
Pro	42	63	66	1.0	20.8	0.57	0.66
Ala	40			0.5		1.42	1.07
Arg	40	62	63	0.2	49.6	0.98	1.03
Asp	42	63	65	1.1	38.4	1.01	0.68
Cys	41			0.7	35.4	0.70	0.92
Gly	40	62		0.7		0.57	0.59
His	40		62	0.7	67.5	1.00	0.69
Ile	40			0.7		1.08	1.14
Leu	40			0.5	41.2	1.21	1.14
Ser	41			0.7	27.5	0.77	0.76
Thr	41			0.8		0.83	0.82

*Activity was measured as the relative amount of enzyme required to give a cleared area with a radius of 7.0 mm in the lysoplate assay of Becktel and Baase (*18*). Each plate contained 0.65 g of purified *Escherichia coli* peptidoglycan in 5% glycerol, 120 m*M* potassium chloride, 20 m*M* phosphate, *p*H 6.8. The assay was carried out for 24 hours at 5°C.

Institute of Molecular Biology and Department of Physics, University of Oregon, Eugene, OR 97403.

ty maps with coefficients ($F_{mutant} - F_{WT}$) and ($2F_{mutant} - F_{WT}$) and phases of the refined structure of the wild-type enzyme (*21*) were calculated for all seven mutants.

A starting model for each mutant lysozyme was obtained by adapting the coordinates of the wild-type enzyme (*21*) or of the Gly[86] mutant protein with the program FRODO (*22*). Crystallographic refinement (*23*) was started by making positional adjustments with loose restraints of bond angles (7° to 8°) and bond lengths (0.06 to 0.07 Å). After refinement of temperature factors, the geometrical restraints were tightened to limit deviations from expected bond lengths (0.02 Å) and angles (2° to 3°). Finally, the thermal parameters were allowed to vary to yield the final parameter sets (Table 2; coordinates submitted to Brookhaven Data Bank).

Table 2. Data collection and refinement statistics. See Table 3 for an explanation of the Gly (1) and Gly (2) structures.

Residue 86	Pro	Arg	Asp	Cys	Gly (1)	Gly (2)	His	Leu	Ser
Data collection									
Films	28	15	18	20	28		19	16	19
Total measurements	70,200	33,800	37,600	40,400	57,200		40,200	31,600	38,600
R_{merge} (%)	14.3	7.3	6.5	8.4	9.0		7.0	7.0	6.1
Cell dimensions									
a, *b* (Å)	61.2	61.2	61.2	61.2	61.2		61.2	61.2	61.2
c (Å)	96.8	96.8	96.8	96.9	96.8		97.1	96.8	96.9
Refinement									
Resolution (Å)	1.7	1.8	1.8	1.7	1.9		1.7	1.7	1.7
Independent reflections	16,909	13,359	14,235	15,397	13,472		15,695	15,087	14,592
R_{refine} (%)	18.7	17.3	17.0	18.4	16.9	16.8	17.8	17.5	18.1
Root-mean-square deviation from ideal stereochemistry									
Bond length (Å)	0.020	0.019	0.019	0.019	0.020	0.019	0.018	0.019	0.019
Bond angles (degrees)	2.84	2.93	2.81	2.75	2.95	3.00	2.95	2.96	2.95
Trigonal atom planarity (Å)	0.022	0.020	0.019	0.018	0.021	0.023	0.021	0.021	0.020
Group planarity (Å)	0.024	0.023	0.023	0.021	0.023	0.024	0.021	0.024	0.019

Table 3. Interatomic distances in α-helical region 81 to 91. The distances quoted are between carbonyl oxygens and amide nitrogens of residues 81 to 91 of wild-type and six mutant lysozymes. The first six entries for main-chain atoms are α-helical ($i + 4$) hydrogen bonds and the last two entries are 3_{10} helical ($i + 3$) hydrogen bonds. Pro[86] in the wild-type protein blocks intramolecular hydrogen bonds to the carbonyl oxygens of residues 82 and 83 (marked with *). To determine if the hydrogen bond distances reflect a bias from the starting coordinates, a model of the protein with Gly[86] built into a more regular α-helix was subjected to crystallographic refinement. [The initial refinement, Gly (1), started with a model more similar to the wild-type protein.] Crystallographic refinement of both starting models produced essentially the same final coordinates. As shown in the table, the distances from the carbonyl oxygens of residues 82 and 83 to the amide nitrogens of 86 and 87 are essentially identical in the independently refined structures of the variants Gly (1) and Gly (2). The distortions of this helical segment observed in the mutant proteins are apparently not artifacts of the initial molecular model. The "side-chain" hydrogen bond is at the amino terminus of the helix between the peptide nitrogen of residue 83 and the side chain carbonyl oxygen of Asn[81].

Residue pairs	Distance between atom pairs for various amino acids at position 86 (Å)								Average (± SD) over all mutants (Å)
	Pro	Arg	Asp	Gly (1)	Gly (2)	His	Leu	Ser	
Main chain									
81, 85	2.8	2.8	2.8	2.8	2.8	2.8	2.8	2.7	2.79 ± 0.04
82, 86	4.7*	3.2	3.1	3.5	3.4	3.3	3.3	3.3	3.30 ± 0.13
83, 87	4.4*	3.5	3.4	3.7	3.7	3.5	3.4	3.6	3.54 ± 0.13
84, 88	3.0	2.9	2.9	3.0	3.0	3.0	2.9	3.0	2.96 ± 0.05
85, 89	2.9	2.8	3.0	2.9	2.9	2.9	2.9	2.9	2.90 ± 0.06
86, 90	3.2	3.3	3.4	3.4	3.3	3.4	3.4	3.4	3.37 ± 0.05
87, 90	3.0	3.0	2.9	3.0	3.0	2.9	2.9	2.9	2.94 ± 0.05
88, 91	3.2	3.0	3.1	3.1	3.1	3.1	3.1	3.0	3.07 ± 0.05
Side chain									
81, 83	2.8	3.2	3.3	3.1	3.1	3.1	3.2	3.0	3.14 ± 0.10

Pro[86] is on the surface of T4 lysozyme in a helix at the beginning of the COOH-terminal domain. The carbonyl oxygens of residues 81 and 84 to 86 are within hydrogen-bonding distance of the amides of the $i + 4$ amino acids, characteristic of an α-helix, and residues 87 to 91 form a 3_{10} helix (Table 3). The side chains of Asn[81] and Arg[96] form hydrogen bonds to the amide and carbonyl groups at the helix termini. The side chains of Leu[84], Val[87], and Leu[91] anchor this segment to the protein by protruding into the hydrophobic core of the COOH-terminal domain. Pro[86] blocks the formation of a continuous helix through this region. The pyrrolidine ring forces the carbonyl oxygens of Ala[82] and Lys[83] to tilt away from the helix axis toward the solvent.

X-ray structural studies of seven lysozymes with replacements of Pro[86] indicate that the mutations cause a similar structural change. As an example, the difference in electron density between the proteins with Gly and Pro (WT) at position 86 is shown in Fig. 1. Negative density due to the loss of the proline side chain is accompanied by paired positive and negative features that indicate substantial shifts of Ala[82] and Lys[83]. The carbonyl groups of these two residues tilt toward the helix axis into the space vacated by the pyrrolidine ring. The side chain of Asn[81] on the protein surface follows this shift while maintaining its contacts with the neighboring side chain of Glu[108]. Other amino acids in contact with this region (including 109 to 112) and residue 86, the site of the amino acid substitution, do not shift. Comparison of the refined coordinates of the wild-type and Gly[86]-mutant proteins shows that the largest changes in the coordinates occur in residues 81 to 83 and the associated solvent (Fig. 2). The carbonyl oxygens of amino acids 82 and 83 shift ~1.4 and 1.0 Å, respectively, and the side chain of Asn[81] moves ~0.4 Å. In the wild-type protein the side-chain amide of Asn[81] is more than 11 Å from the site of the amino acid replacement.

Difference maps and crystallographic refinements of the structures of the lysozymes with Ser, Leu, Asp, Arg, and His at position 86 show structural changes similar to those described for the Gly[86] variant. Shift plots comparing the backbone atoms of one mutant protein with another show much smaller differences than comparisons of each of the variants with the wild-type lysozyme (Fig. 2). The similarity of the main-chain conformations of six of the mutant lysozymes is highlighted in Fig. 3, which shows the refined models of residues 81 to 88 of the mutant and wild-type proteins superimposed.

The conformational changes in the mu-

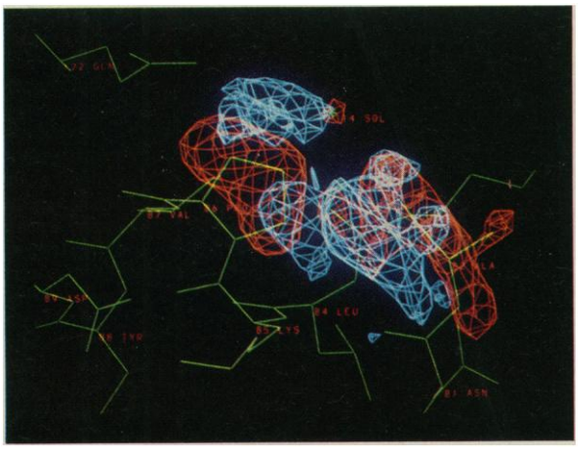

Fig. 1. Difference in electron density due to the substitution Pro[86] → Gly superimposed on the model of wild-type lysozyme. The map was calculated to a resolution of 1.9 Å with coefficients ($F_{Gly} - F_{Pro(WT)}$) and phases of the refined structure of the wild-type protein. Positive features are in blue and negative features are in red. The contour level is 4σ, where σ is the root-mean-square electron density in the unit cell. The pyrrolidine ring of Pro[86] is clearly absent from the mutant protein, and the movement of the main chain of residues 81 to 83 is apparent. For clarity, only the vicinity of the mutation is shown.

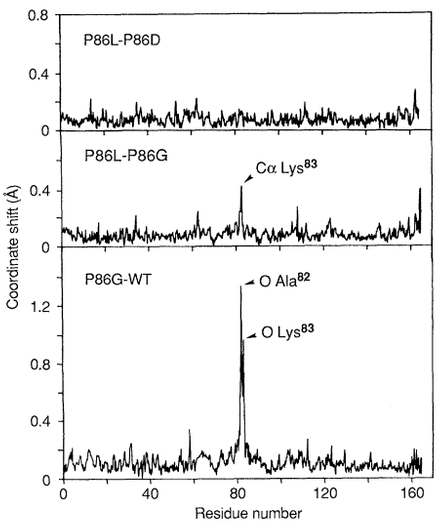

Fig. 2. Shift plots showing the differences in the refined coordinates of all common atoms of wild-type and representative mutant lysozymes. Three pairs of structures, denoted by the one letter code for the amino acids, are compared. The mutant proteins P86L (Pro[86] → Leu), P86D (Pro[86] → Asp), and P86G (Pro[86] → Gly) are more similar to each other than to the wild-type enzyme. Atoms with the largest coordinate shifts are labeled.

tant lysozymes result in the formation of a continuous helix that includes residues 81 to 91. The helix is distorted, however, because the two new intrahelical hydrogen bonds to the carbonyl oxygens of Ala[82] and Lys[83] are unusually long (Table 3).

The positional shifts of residues 81 to 83 are associated with significant increases in the crystallographic thermal factors (Fig. 4). The average *B* values of the main-chain atoms of residues 82 and 83 in the Pro[86] → Gly mutant rise from 24 Å^2 and 21 Å^2 to 37 Å^2 and 30 Å^2, respectively. A similar increase in main-chain *B* values occurs in all of the mutant proteins (Fig. 4).

The position and dynamics of the backbone atoms of residue 86 are insensitive to the amino acid substitutions, despite the fact that the side chains at this site adopt different average conformations and make different intramolecular contacts (Fig. 3). The hydroxyl group of Ser[86], for example, is within hydrogen-bonding distance of the side chain of Gln[122]. Gln[122] moves toward Ser[86] to make this contact. Cys[86] makes an analogous hydrogen bond, but the bulkier SH group pushes Gln[122] away from the site of the mutation. The imidazole ring of His[86] is within 3.0 Å of the carbonyl oxygen of Ala[82], although the angle between these groups (92°) does not favor the formation of a strong hydrogen bond. The side chains of Asp and Arg do not form specific polar interactions with neighboring groups. At *p*H 6.0 and 65°C, Asp[86] stabilizes the protein by ~0.7 kcal/mol compared to Arg[86]. At *p*H 2, the maximum difference in the stabilities of the mutant lysozymes is 0.25 to 0.5 kcal/mol at 42°C (Table 1) (*17*). This suggests that long-range ionic interactions lead to a difference in stability of less than 0.5 kcal/mol. The new side chains at position 86 are more disordered than the wild-type proline (Table 1). The lower mobility of Pro[86] may reflect the constraints imposed by covalent bonds in the pyrrolidine ring. The hydrogen bond to the side chain of Ser[86] may also be responsible for its reduced thermal parameter.

Due to restriction of the φ torsion angle and the increased occurrence of the cis isomer, proline can play special roles in the folding (*24*) and the stabilization (*25*) of proteins. None of the ten proline substitutions reported here blocks the folding of phage lysozyme. The substitutions cause substantial conformational changes, but the thermal stabilities of the mutant proteins are only marginally lowered.

These results emphasize that proteins can be surprisingly tolerant of amino acid substitutions (*26*). One mechanism by which this occurs is that the native structure (and presumably the unfolded state as well) can adjust to accommodate changes in sequence. Substitution of Pro[86] causes one of the most extensive conformational changes observed in the mutants of lysozyme analyzed to date. Structural differences propagate across the protein surface from Gln[122] to water 316 and Glu[108], a distance of over 20 Å. Such changes in structure can mitigate the intrinsic energetic effects of mutations.

Flexibility allows proteins to be more tolerant of mutations. If proteins were completely rigid, changes in amino acid sequence would have a larger impact on the free energy of the folded state and on thermodynamic stability. The effects of a given substitution on the free energies of the folded and unfolded states may depend on the intrinsic effects of the change and on the relative abilities of the two states to structurally compensate for the new amino acid; the most rigid amino acids in the x-ray crystal structure of phage T4 lysozyme are also the most sensitive to severe destabilizing substitutions (*27*). Rigid parts of the folded conformation may be least able to compensate for changes.

A striking aspect of the substitutions of Pro[86] is that the extension of the helix to include two additional residues does not stabilize the mutant lysozymes. The x-ray structural studies are consistent with at least two underlying explanations. First, the new intrahelical interactions in the mutant proteins may be no more stabilizing than interactions (with solvent) in the wild-type enzyme. In the mutant structures, the carbonyl oxygens of residues 82 and 83 each move ~1 Å to approach the new amide at position 86 and the amide of Val[87]. These pairs of amide and carbonyl groups, however, are on average still 3.3 and 3.5 Å apart (Table 3). These distances are longer than the hydrogen-bond distance of 3.0 Å in an ideal α-helix and outside the range of 2.7 to 3.2 Å seen for the separation of hydrogen-bonded amides and carbonyls in crystal structures of small molecules (*28*). As a result, the two new intrahelical hydrogen bonds in the mutant proteins may contribute little to stability.

A second possibility is that the extended helix is more stable, but it interacts less well with the remainder of the structure. The contacts of the side chain of Asn[81], for example, provide support for this view. In wild-type T4 lysozyme, the side-chain carbonyl oxygen is 3.0, 2.8, and 3.2 Å, respectively, from the amides of residues 82 to 84. In the mutant proteins, these distances increase to 3.1, 3.1, and 3.5 Å, respectively. This suggests that the hydrogen bonds to the new helix terminus are weaker in the mutant structures.

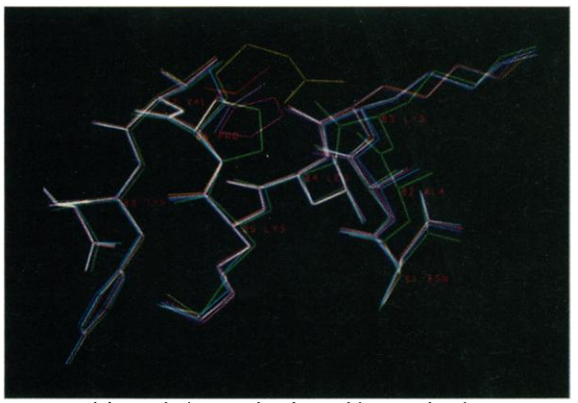

Fig. 3. Superposition of the refined structures of wild-type lysozyme (green) and variants with Gly (navy), Ser (light blue), Leu (red), Asp (violet), Arg (yellow), and His (pink) at position 86. Residues 81 to 87 are shown. These six amino acid substitutions cause a similar shift in the backbone conformation of residues 81 to 83. With Cys at residue 86, the position of the backbone of residues 81 to 83 is intermediate between the conformations observed in the wild-type and in the other mutant proteins. About 40% of the Cys^{86} residues in the crystalline protein form an adduct with 2-mercaptoethanol, which in turn participates in intramolecular and intermolecular contacts. Because these interactions could influence nearby atoms, the structure of the Cys^{86} variant is not included in the figure (or in Table 3).

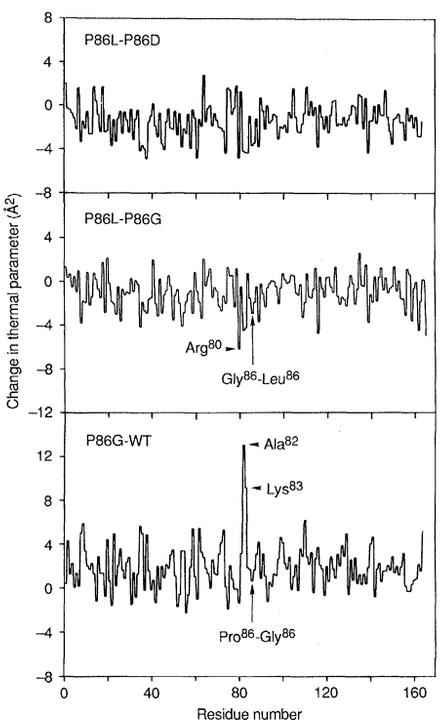

Fig. 4. Differences in the average thermal parameters of the main-chain atoms of wild-type and representative mutant lysozymes. *B*-values of nitrogen, α-carbon, carbonyl carbon, and oxygen atoms of each residue were averaged and pairwise differences were plotted as a function of residue number. Comparisons of the refined coordinates of these lysozyme variants are shown in Fig. 2. As in Fig. 2, the amino acid substitutions in the mutant proteins are indicated by the one letter code. An increase in *B* of 8 to 12 $Å^2$ for the backbone atoms of residues 82 and 83 occurs in the mutant lysozymes with Leu, Asp, and Gly (as well as those with His, Arg, and Ser) at position 86.

Comparisons of wild-type T4 lysozyme with the mutant proteins are complicated by their conformational differences. The mutant proteins, though, are similar to each other (Fig. 2 and 3). They differ mainly in the conformation of the altered side chain. Ser, Cys, and His make polar contacts that obviously cannot be made by the nonpolar residues, and buried hydrophobic surface area differs from side chain to side chain. In addition, Arg and Asp have opposite charges. Given these structural differences, it is surprising that amino acid substitutions at position 86 have little effect on the stability of the protein (Table 1). The stabilizing contributions of these side chains at position 86 apparently are very small or are easily compensated.

Some interactions inferred from the x-ray crystal structure (for example, the hydrogen bond between Ser^{86} and Gln^{122}) do not correlate with increased stability. In this instance the additional intramolecular hydrogen bond may mimic interactions with solvent and contribute equally to the free energy of the folded and unfolded states (*29*). Pro^{86} is largely solvent exposed and the thermal parameters of the new side chains at this position are all higher than average (Table 1). Consequently, the environment and the energetic contribution of residue 86 may be similar in the folded and unfolded states. This idea is consistent with the finding that amino acid substitutions with dramatic effects on stability do not generally occur at residues that are solvent-exposed or mobile in the folded protein (*27*). To account quantitatively for such differential energetic contributions presents a challenge for computational approaches to the protein stability problem.

The ten mutant lysozymes differ widely in the helical propensity of the residue at position 86. By scales based on the normalized frequencies of occurrence in protein helices (*4*) or on host-guest data from model helices (*3*), the amino acids at position 86 include helix formers and helix breakers (Table 1). Nonetheless, within the error of the measurements of T_m (±1°), helix formers and helix breakers stabilize the protein equally well. This suggests that the intrinsic effects of changes in the Zimm-Bragg σ and *s* values at a single residue in a protein can be small or can be easily modified by specific interactions. Direct studies of the effects of amino acid substitutions on the helix formed by the isolated S-peptide of ribonuclease have led to similar conclusions (*9, 10*). The decrease in helical propensity often associated with destabilizing mutations (*6, 7*) could be a fortuitous consequence of the higher-than-average helical propensity of amino acids in protein helices. (The average P_α for helical residues in T4 lysozyme is 1.09. For nonhelical residues, the average P_α is 0.92 (*6*).)

It should be emphasized, however, that residues 81 to 91 do not form an ideal helix in wild-type T4 lysozyme or in the seven mutant proteins whose structures have been determined. The deviations from nonideality in the vicinity of residue 86 in T4 lysozyme may undermine the relevance of scales of helix-forming potential for understanding the effects of mutations in this region.

Comparison of the refined x-ray crystal structures of the enzymatically most active (Pro^{86} → Asp) and least active (Pro^{86} → Arg) variants reveals no significant differences in their active sites. The reduction in enzyme activity of the Pro^{86} → Arg mutant lysozyme may be linked to the addition of a positive charge. An even more severe reduction in activity is caused by the replacement of Glu^{128} by Lys (*30*). Like Pro^{86}, Glu^{128} is far from the active site on the surface of the COOH-terminal domain. The similarity of the effects of increasing the positive charge at these sites may reflect extended interactions of the natural peptidoglycan substrate with the COOH-terminal lobe (*30*), changes in the *p*H dependence of activity, or sensitivity of the transition state to the overall electrostatic potential.

The results reported here emphasize the importance of studying structure, activity, and stability in order to understand the properties of mutant proteins. It is encouraging that even variants with relatively large conformational differences can be subjected to crystallographic analysis.

REFERENCES AND NOTES

1. W. Kauzmann, *Adv. Protein Chem.* **14**, 1 (1959).
2. T. E. Creighton, *Proteins* (Freeman, New York, 1983).
3. H. A. Scheraga, *Pure Appl. Chem.* **50**, 315 (1978); M. Sueki *et al.*, *Macromolecules* **17**, 148 (1984).
4. P. Y. Chou and G. D. Fasman, *Annu. Rev. Biochem.* **47**, 251 (1978).
5. C. Mitchinson and R. L. Baldwin, *Proteins* **1**, 23 (1986).
6. T. Alber *et al.*, *Protein Structure, Folding and Design*, vol. 39. of the *UCLA Symposia Series on Molecular and Cellular Biology* (Liss, New York, 1986), p. 307.
7. M. H. Hecht, J. M. Sturtevant, R. T. Sauer, *Proteins*

1, 43 (1986); M. H. Hecht, K. M. Hehir, H. C. M. Nelson, J. M. Sturtevant, R. T. Sauer, *J. Cell. Biochem.* **29**, 217 (1985).
8. D. Shortle and B. Lin, *Genetics* **110**, 539 (1985).
9. K. R. Shoemaker *et al.*, *Proc. Natl. Acad. Sci. U.S.A.* **82**, 2349 (1985); K. R. Shoemaker, P. S. Kim, E. J. York, J. M. Stewart, R. L. Baldwin, *Nature (London)* **326**, 563 (1987).
10. P. S. Kim and R. L. Baldwin, *Nature (London)* **307**, 329 (1984).
11. T. Alber and B. W. Matthews, *Methods Enzymol.* **154**, 511 (1987).
12. M. J. Zoller and M. Smith, *DNA* **3**, 479 (1984).
13. F. Sanger, S. Nickelsen, A. R. Coulson, *Proc. Natl. Acad. Sci. U.S.A.* **74**, 5463 (1977).
14. U. K. Laemmli, *Nature (London)* **227**, 680 (1970).
15. W. Wray, T. Boulikas, V. P. Wray, R. Hancock, *Anal. Biochem.* **118**, 197 (1981).
16. M. Elwell and J. A. Schellman, *Biochim. Biophys. Acta* **386**, 309 (1975); *ibid.* **580**, 327 (1979); J. A. Schellman, M. Lindorfer, R. Hawkes, M. Grutter, *Biopolymers* **20**, 1989 (1981); R. Hawkes, M. G. Grutter, J. Schellman, *J. Mol. Biol.* **175**, 195 (1984); W. J. Becktel and W. A. Baase, *Biopolymers* **26**, 619 (1987).
17. W. J. Becktel and J. A. Schellman, *Biopolymers* **26**, 1859 (1987).
18. ——— and W. A. Baase, *Anal. Biochem.* **150**, 258 (1985).
19. S. J. Remington *et al.*, *J. Mol. Biol.* **118**, 81 (1978).
20. M. F. Schmid *et al.*, *Acta Crystallogr.* **A37**, 701 (1981).
21. L. H. Weaver and B. W. Matthews, *J. Mol. Biol.* **193**, 189 (1987).
22. T. A. Jones, in *Crystallographic Computing*, D. Sayre, Ed. (Oxford Univ. Press, Oxford, 1982), p. 303.
23. D. E. Tronrud, L. F. Ten Eyck, B. W. Matthews, *Acta Crystallogr.* **A43**, 489 (1987).
24. P. S. Kim and R. L. Baldwin, *Annu. Rev. Biochem.* **51**, 459 (1982).
25. B. W. Matthews, H. Nicholson, W. J. Becktel, *Proc. Natl. Acad. Sci. U.S.A.* **84**, 6663 (1987).
26. T. Alber *et al.*, *Nature (London)* **330**, 41 (1987).
27. T. Alber, S. Dao-pin, J. A. Nye, D. C. Muchmore, B. W. Matthews, *Biochemistry* **26**, 3754 (1987).
28. E. N. Baker and R. E. Hubbard, *Prog. Biophys. Mol. Biol.* **44**, 97 (1984); C. Ramakrishnan and N. Prasad, *Int. J. Protein Res.* **3**, 209 (1971).
29. I. M. Klotz and J. S. Franzen, *J. Am. Chem. Soc.* **84**, 3461 (1962).
30. M. G. Grutter and B. W. Matthews, *J. Mol. Biol.* **154**, 525 (1982).
31. We thank D. C. Muchmore and F. W. Dahlquist for the lysozyme expression system and J. A. Schellman, W. Becktel, and W. Baase for facilities and advice concerning the thermodynamic measurements, L. H. Weaver for help with x-ray data collection, D. E. Tronrud and T. M. Gray for advice on crystallographic refinement, and S. J. Remington for help with graphics. T.A. thanks the Helen Hay Whitney Foundation and J.A.B. thanks the National Institutes of Health for postdoctoral fellowship support. The work was supported in part by grants from the National Institutes of Health (GM 21967 and GM 20066) and the National Science Foundation (DMB 8611084 to B.W.M.; DMB 8609113 to J. A. Schellman).

13 August 1987; accepted 23 November 1987

Labeling of Neural Cells by Gold-Filled Sendai Virus Envelopes Before Intracerebral Transplantation

SUSAN C. ARDIZZONI, ALLAN MICHAELS, GARY W. ARENDASH*

Gold-filled Sendai virus envelopes were fused with cell suspensions from the basal forebrain of fetal rat donors, and the resulting gold-labeled cells were transplanted into the neocortex of adult rat recipients. Not only did large numbers of labeled cells remain intact through 3 months in the neocortex, but sizable numbers migrated subcortically to the recipient's lesioned nucleus basalis region (a distance of 4 to 5 millimeters). Since this technique is capable of labeling most transplanted cells for long periods of time, it may be useful in determining the survival, migration, and connectivity of intracerebrally transplanted tissues.

INTRACEREBRAL TRANSPLANTATION IS well established as an important technique in neuroscience (*1, 2*). For a number of grafting studies, an ability to label neural cell suspensions before transplantation is highly desirable in monitoring the survival, differentiation, and possible migration of transplanted cells. The techniques currently in use involve either fluorescent dye or autoradiographic labeling (*3*). However, these techniques have certain drawbacks, such as the diffusion of dye markers out of neurons after several weeks. We describe a method for labeling neuronal cell suspensions with Sendai virus envelopes that is rapid, capable of labeling most cells, and apparently long-lasting without causing obvious harm to the transplanted cells. Furthermore, we report on the use of this labeling procedure in determining the survival of transplanted fetal rat cells from the nucleus basalis region and their capacity to migrate after intracortical transplantation.

Sendai virus is highly fusogenic to most vertebrate cells and is nonpathogenic to man. The fusion activities of this virus are due mainly to two viral glycoproteins located in the viral envelope. Viral envelopes were obtained by solubilization of intact Sendai virus with the detergent Triton X-100, followed by removal of the detergent through slow dialysis to reconstitute the glycoproteins and lipids into envelopes that are structurally and biologically similar to Sendai virus envelopes (*4, 5*). During the reconstitution process, the viral nucleocapsid was removed and replaced by exogenous colloidal gold particles that became trapped within the reassembled viral envelopes during dialysis. These reassembled viral envelopes were then used as biological syringes to inject colloidal gold into neurons and glial cells during viral envelope–cell fusion.

Colloidal gold–containing Sendai virus envelopes were prepared from Sendai (Cantell) hemagglutinin (Hazleton Research Products, Denver, Pennsylvania) by using modifications of a general procedure by Volsky and Loyter (*5, 6*). Previously frozen or freshly prepared nucleus basalis magnocellularis (nBM) cell suspensions from dissected fetal rat brains (day 18 of gestation) were prepared (*7*) and fused with the colloidal gold–containing viral envelopes (*8*). More than half of the cells within a given nBM suspension were labeled, although we have routinely achieved nearly 100% labeling. Two microliters of this labeled nBM suspension were then transplanted unilaterally into four frontoparietal cortex sites of adult Sprague-Dawley rats (*9*) that had received an ipsilateral excitotoxic lesion of the nBM region 1 to 3 weeks earlier (*10*). Recipients were killed at 10 days, 30 days, or 3 months after transplantation, and their brains were histologically prepared (*11*).

Because of a small, unavoidable contamination of labeled cell suspensions by residual free colloidal gold or unfused gold-containing envelopes, control infusions of either colloidal gold or gold-containing capsules were performed to determine if these contaminants would be taken in by surrounding cells. Results indicate that only a small number of cells near the cortical infusion area (most probably glia and pial cells) will take up free colloidal gold or fuse with reconstituted viral envelopes. Furthermore, the limited number of cells that do take up one of these control infusates remain in the infusion area. It is unlikely that labeled cells are host cells that have phagocytized degenerating transplanted cells since no cellular labeling was observed at infusion sites in two animals with necrotic, nonviable transplants (that is, the colloidal gold released from degenerative transplanted cells was apparently cleared from the brain).

Through 3 months after transplantation, large numbers of grafted, gold-labeled cells were seen at neocortical infusion sites (Fig. 1), although markedly more labeled cells were present at these sites when the nBM

S. C. Ardizzoni, Department of Biology, University of South Florida, Tampa, FL 33620.
A. Michaels, Biology Department, Ben Gurion University of the Negev, Beersheba 84105, Israel.
G. W. Arendash, Department of Biology, University of South Florida, Tampa, FL 33620, and Department of Neurology, University of South Florida College of Medicine, Tampa, FL 33612.

*To whom correspondence should be addressed.